Ti6Al7Nb SURFACE MODIFICATION BY ANODIZATION IN ELECTROLYTES CONTAINING HF

Emanuela-Daniela STOICA[1], Fedor FEDOROV[2], Maria NICOLAE[3], Margitta UHLEMANN[4], Annett GEBERT[5], Ludwig SCHULTZ[6]

Lucrarea de faţă prezintă unui studiu privind modificarea suprafeţei de Ti6Al7Nb prin anodizare în electroliţi conţinând HF, cu scopul de a obţine un strat de oxid poros. Caracterizarea microstructurală şi stabilitatea la coroziune a substratului de Ti6Al7Nb au fost realizate prin microscopie electronică cu baleiaj, difracţie de raze X şi măsurători de polarizare potenţiodinamică. Anodizare s-a efectuat în doi electroliţi ce conţin diverse concentraţii de HF la diferite durate de anodizare. Suprafeţele anodizate au fost analizate prin microscopie electronică cu baleiaj, astfel stabilindu-se condiţiile optime investigate pentru formare unui strat de oxid nanotubular.

The present paper addresses a study of Ti6Al7Nb surface modification by anodization in electrolytes containing HF, with the purpose to achieve an ordered porous oxide layer. The microstructural characterization and corrosion stability of Ti6Al7Nb substrate were achieved by scanning electron microscopy, X-ray diffractometry and potentiodynamic polarization measurements. The anodization was performed in two electrolytes with different HF concentration at different anodization time. The anodized surfaces were analyzed by scanning electron microscopy; hence the optimal investigated conditions for nanotubular oxide layer formation were established.

Keywords: titanium alloys, oxide nanotubes, anodization

1. Introduction

Titanium and its alloys are the most used metallic materials for biomedical applications, due to their excellent mechanical, biological and chemical

[1] PhD student, Materials Science and Engineering Faculty, University POLITEHNICA of Bucharest, Romania, e-mail: stoicaemanueladaniela@yahoo.com

[2] PostDoc, Institute for Metallic Materials, IFW Dresden, Germany

[3] Prof., Materials Science and Engineering Faculty, University POLITEHNICA of Bucharest, Romania

[4] Senior Scientist, Department Electrochemical Properties of Functional Materials, Institute for Metallic Materials, IFW Dresden

[5] Head of Department, Dept. Electrochemical Properties of Functional Materials, Institute for Metallic Materials, IFW Dresden, Germany

[6] Director of the Institute for Metallic Materials, Director of IFW Dresden

properties. Ti6Al7Nb and Ti6Al4V are probably the best known titanium alloys and they are meanwhile well-established metallic materials for implants, especially on replacement of hip joints [1].

Ti6Al7Nb is an alpha-beta titanium alloy with good corrosion resistance, clinically used since 1986 [2]. Like all the titanium alloys, its biocompatibility is mainly related to the phenomenon of a spontaneously forming thin adherent TiO_2 layer (about 5-20nm thickness) which covers naturally its surface. Besides TiO_2 this passive film contains oxides of the alloying elements (Al and Nb are known as valve metals [3]), in this case Al_2O_3 and Nb_2O_5. The Ti6Al7Nb alloy is more biocompatible than Ti6Al4V, due to formation of Nb_2O_5 which is in body fluids chemically more stable and less soluble than V_2O_5 [1]. Since this material Ti6Al7Nb was a very often research subject in many studies it became a "classic" metallic biomaterial [2, 4-7].

In the last years, the studies in the biomaterial field are focused on two directions. The first one is the development of new metallic materials with mechanical properties closer to those of the human bone e.g. single phase beta type Ti alloys [8-10]. The second direction is devoted to new surface modification techniques enabling optimum osseointegration of the Ti alloy implant. Different methods were established like mechanical (blasting, machining,), chemical (electrochemical treatment, alkaline treatment, acidic treatment) and physical treatments (ion implantation, physical vapor deposition [11])

The anodic oxidation (anodization) in electrolytes containing fluoride ions is a new electrochemical method for surface modification. Using this technique for titanium and its alloys, a porous oxide layers can be achieved [7-13]. In general, the electrolytes employed for the anodization process of Ti6Al7Nb are: $(NH_4)_2SO_4$ solutions or H_3PO_4 solutions with different amounts of NH_4F [7-12] or HF [14].

The present study on Ti6Al7Nb samples is focused to obtain nanotubular oxide layers using the anodization technique in HF mixtures with H_3PO_4 and to characterize the layer properties in dependence on the electrolyte composition and anodization time.

2. Materials and methods

2.1. Alloy preparation and characterization

The cast alloy Ti6Al7Nb disks (2 mm thickness and 11 mm diameter) were microstructurally investigated before the anodization process. These samples were metallographically prepared and the polished surfaces were etched in a solution of 2% HF for a couple of seconds and subsequently analyzed using scanning electron microscopy (SEM). Furthermore the samples were subjected to

the x-ray diffraction analysis (XRD). The chemical composition of cast alloy samples was determined using inductively coupled plasma optical emission spectrometry analysis (ICP-OES). A very good agreement with the nominal composition was revealed.

Corrosion tests were performed by means of potentiodynamic polarization measurements in Ringer's solution (8 g/l NaCl, 0,2 g/l KCl, 0,2 g/l $CaCl_2$, 1 g/l $NaHCO_3$) with, a pH value of ~ 7,4 (adjusted with 10% HCl) at 37^0C using a potential sweep rate of 0.5 mV/s. The electrochemical corrosion cell consisted of a platinum foil as counter electrode, a saturated calomel electrode (SCE) with E (SCE) = 0.241 V vs. NHE as reference electrode and a Ti6Al7Nb polished disk sample as working electrode. These potentiodynamic polarization tests were conducted also for Ti and Ti6Al4V samples in order to compare the corrosion parameters E_{corr} ,i_{corr} and i_{pass} .

2.2. Electrochemical anodization treatment

Prior to anodization treatments the Ti6Al7Nb disks were ground with emery papers grit 600, 800, 1200 and 2500, polished with 6μm diamond paste and cleaned by sonication in ethanol and distillated water for 10 minutes. The electrochemical cell consisted of a two-electrode configuration with platinum foil as a counter electrode and Ti6Al7Nb sample as working electrode with a 0.282 cm^2 surface area exposed to the electrolyte. The anodization experiments were carried out using a high-voltage potentiostat 2400 Source Meter Keithley connected to a digital multimeter (Keithley 2700 Multimeter /Data Acquisition System) interfaced to a computer. The samples were anodized in 1 M H_3PO_4 solution with addition of 0.1 wt. % HF and 0.2 wt. % HF at room temperature (pH ~2) [6]. The anodization treatment comprised a potential ramp from open circuit potential (OCP) to 20 V with a sweep rate of 20 mV/s. The applied sweep rate was found to be the most appropriate for nanotubes formation on α+β titanium alloys in electrolyte with NH_4F content [7]. The potential of 20 V was held constant for 40 minutes, 1 hour and 2 hour in each electrolyte. After the anodization treatment all samples were rinsed in distilled water and dried.

The structural and morphological characterization of the oxide layers was carried out with the Leo 1530 Scanning Electron Microscope (SEM).

3. Results and discussion

3.1. Alloy characterization

The electrochemical response of an alloy is principally determined by its microstructure characteristics. Therefore, in first step a detailed analysis of the

Ti6Al7Nb substrates was conducted by means of SEM and XRD. Fig.1. shows an SEM image in composition of an HF etched cross-sectional area of a Ti6Al7Nb disk sample. The typical Ti6Al7Nb microstructure is clearly revealed with both phases α and β. The α-phase corresponds to the dark contrast areas and the β-phase to the bright areas. It can be assumed that the α-phase contains the Al element while the β-phase comprises the Nb element. This knowledge on the phase distribution is decisive for the following studies since according to literature [6,7,12, 14] in solutions containing HF the electrochemical behaviors of the α and β-phases may be different.

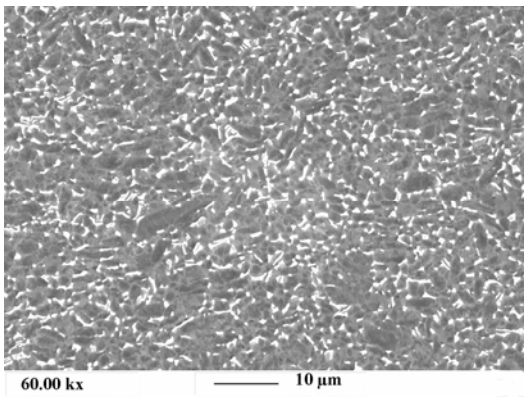

Fig.1. SEM images (BSE mode) of a Ti6Al7Nb sample cross section
(α phase dark contrast and β phase bright contrast)

The chemical composition of the investigated cast Ti6Al7Nb samples (as determined by ICP-OES) was 6.21 wt. % Al, 7.08 wt. % Nb, 0.13 wt. % Fe, 0.11 wt. % O, 0.032 wt. % N , 0.082 wt. % C, bal. Ti). Thus, it is in very good agreement with the nominal composition.

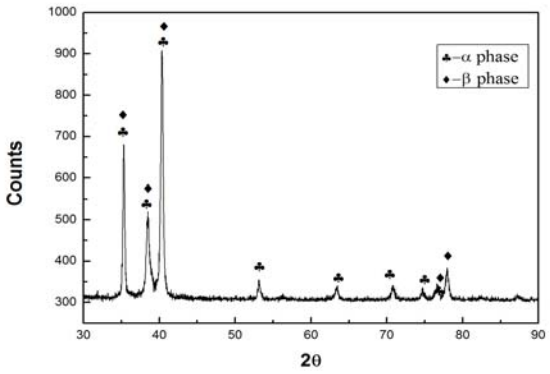

Fig.2. XRD pattern of a Ti6Al7Nb sample

Fig.2. shows a representative XRD pattern for a cast alloy. The XRD data were compared with reference data base codes 01-071-9957 and 04-008-7849 corresponding to Nb, Ti and rutile, respectively. The main reflections correspond to 2θ=40.2°, 2θ=35.1°, 2θ=38.4° and 2θ=77.8° respectively for Ti and Nb phase. The main reflection for rutile was captured at 2θ=27.3°.

3.2. Corrosion tests

In order to evaluate the stability of the cast Ti6Al7Nb samples in a body fluid environment, corrosion studies in artificial Ringer's solution were conducted. The most important data which determine the corrosion behavior of metallic material are in general E_{corr} (corrosion potential), i_{corr} (corrosion current density) and i_{pass} (passive current density). Fig.3 shows a typical potentiodynamic polarization curve for Ti6Al7Nb alloy in Ringer's solution in comparison to curves for Ti and Ti6Al4V.

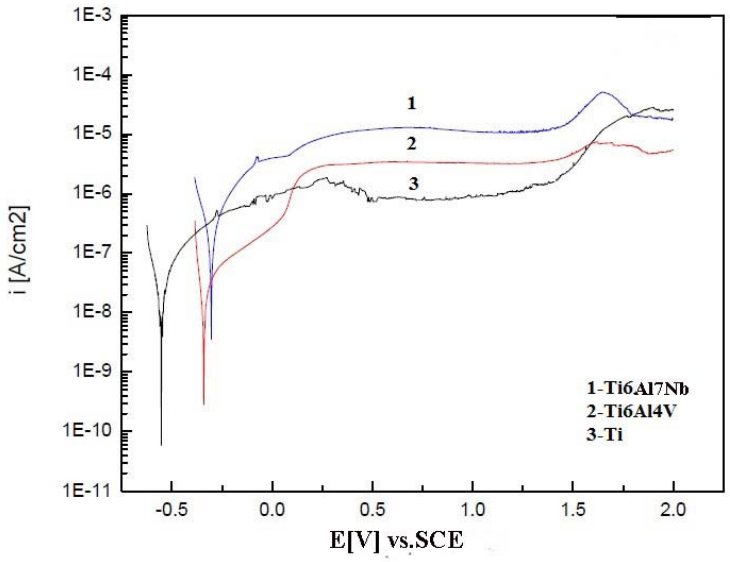

Fig.3. Potentiodynamic polarization curves for Ti6Al7Nb, Ti6Al4V and Ti in Ringer's solution, pH 7, at 37°C

Under quasi-stationary polarization conditions, i.e. at very slow scan rates the initial curve section reflects the "free corrosion behaviour". E_{corr} corresponds to the sharp i-minimum and i_{corr} can be determined by extrapolating the two curve sections. For Ti, E_{corr} is relatively negative. In comparison, for the two alloys E_{corr}

is shifted to more positive values and in particular for Ti6Al7Nb i_{corr} is significantly increased. Table 1 summarizes corrosion data as extracted from the curves.

Upon further anodic polarization all tested materials exhibit a gradual increase of the current density before entering a plateau-like behavior. This is indicative for direct transfer into a wide stable passive regime. Above ~1.2V in all cases a transpassive transition step occurs. In this study the overall passive current density levels are low. The maximum value is not higher than 11μA/cm^2 reflecting the barrier-type character of the oxide layers. No indications for pitting processes are given. However, the passive current density plateaus for Ti6Al7Nb and for Ti6Al4V are higher than that of pure Ti.

Table 1 shows a direct comparison of i_{pass} values for the tested materials at 0.75 V vs. SCE.

Table 1

Corrosion test parameters for Ti, Ti6Al7Nb and Ti6Al4V alloys

Material	*E_{corr} [V]*	*i_{corr} [μ A/cm^2]*	*i_{pass} [μ A/cm^2]*
Ti6Al7Nb	*-0.28*	*0.6*	*10.7*
Ti6Al4V	*-0.34*	*0.03*	*3.3*
Ti	*-0.55*	*0.04*	*0.7*

Adding alloying elements changes the chemistry of the metallic substrate which can cause a positive shift of E_{corr} (due to more noble standard electrode potentials of Nb, V compared to Ti, Al).

However upon alloying a change from single phase (Ti) to multi-phase (α+β) states also takes place. This increased heterogeneity based on phases with different composition and the more defective nature of the grown passive layers can explain the observed increased reactivity of the alloys [16].

Furthermore, also in accordance with literature data it has to be emphasized that the electrochemical response of Ti-based materials in the "low current regime" is very sensitive to the environmental and surface effects. In similar corrosion studies on Ti6Al7Nb samples it was indicated that slight changes of the pH value of the Ringer's solution or a rougher surface finish state obtained by mechanical grinding can lead to significant deviations of the corrosion data [6].

3.3. Anodization treatments

The anodization process was carried out in the high voltage regime. The electrolytes employed were 1 M H_3PO_4/0.1 wt% HF (El.1) and 1 M H_3PO_4/0.2 wt% HF (El.2) [14]. Fig.4. shows typical current transient curves recorded during polarization at 20V for each electrolyte and to comparison, a schematic curve for

α-Ti anodization (inserted in Fig.4). The anodization curves give information about the growth mechanism of TiO_2. In literature the anodization curve for Ti was divided in five principal stages. The first stage corresponds to a compact surface layer formation; the following stage is the partial destruction of the compact oxide layer and the formation of a random porous layer. The last stages (Fig.4. stages 3-5) are related to the nanotubes growth underneath the random porous layer [17-19].

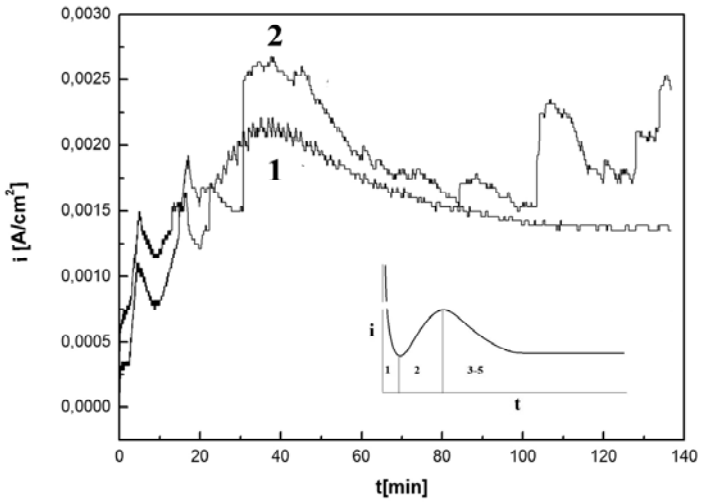

Fig.4. Current transients recorded for Ti6Al7Nb polarization at 20 V and the potential with 20mV/s sweep (1-El.1, 2-El.2)

The shape of the curves is almost similar to the schematic curve for α-Ti, except that for Ti6Al7Nb recorded curves the characteristic first stage cannot be identified and the current density shows some variations. This fluctuation of current density can be related to bubbles formation due to the water decomposition reaction and also to the fact that the subjected material is an alloy with heterogeneous surface structures. Furthermore, the first curve which corresponds to El.1 with lower HF concentration is smoother. Hence, it can be assumed that in a solution with 0.2 wt% of HF the partial current of water decomposition is higher (curve scattering). After 80 minutes anodization in El.2 (curve indexed with 2) the influence of bubbles formation is also significant. This reaction seemed to have a lower impact in the 20-80 minutes region. The shape of the curve within the above mentioned time range can be identified with the stage of pores/tubes formation. It was mentioned in literature that nanotube steps growth on α+β alloys in electrolytes containing fluoride ions occurs with different rates of the electrochemical process on α-and β-phase [12].

3.4. Characterization of the anodized alloys surface

Scanning electron microscopy was employed for the structural and morphological characterization of the Ti6Al7Nb sample surfaces after the anodization process. The SEM image of the alloy surface anodized in 1 M H_3PO_4 /0.1 wt% HF, for 40 minutes (Fig.5) shows that the alloy phases are differently affected by the treatment in fluoride-containing solution. Under these conditions only on the α-phase a porous oxide structure formed, while the β-phase surface was just etched.

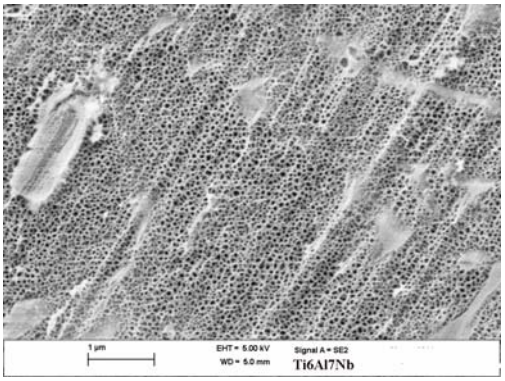

Fig.5. SEM image of Ti6Al7Nb surface after anodization in 1 M H_3PO_4 /0.1 wt% HF, for 40 minutes

When the anodization time was increased up to 1 hour, the structure of the oxide scale seemed to be porous on both phases, but appeared to be in a much more ordered state on the α -phase region (Fig. 6.a,).

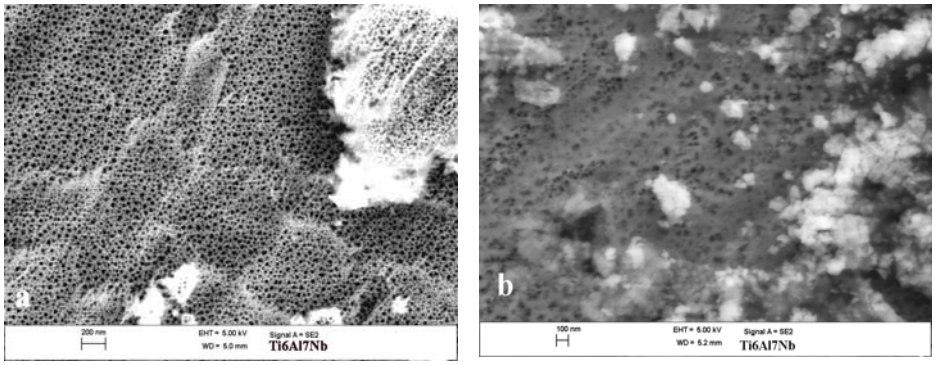

Fig.6. SEM top view α and β phases image of Ti6Al7Nb surface after anodization in 1 M H_3PO_4 / 0.1 wt% HF, for 1 hour (a) and 2 hours (b)

In literature it was already mentioned that the α-phase forms much ordered nanoporous or nanotubular structures [12]. The sample surface was scratched in order to study the dimensional parameters. It was observed that ordered oxide tubes are growing under the random porous surface layer after 1 hour anodization time using 1 M H_3PO_4 + 0.1 wt% HF electrolyte. This phenomenon is attributed to the last stages in the mechanism of TiO_2 growth [15-17]. When the anodization time was increased up to 2 hours only locally non-organized porous structures were observed on the alloy surface (fig.6.b).

For the second electrolyte with higher HF concentration, 1 M H_3PO_4 + 0.2 wt% HF for polarization at 20 V for 40 minutes the same porous structure was achieved for the α-phase (Fig.7 a). Also in this case the β phase seems to be just etched and less wide but did not present any porous structure. Underneath the random porous oxide layer a nanotubular oxide layer was found (Fig.7 b). As it was observed the porous oxide structure on α-phase can be formed within the 40 minutes of anodization in electrolyte with 0.2 wt% HF.

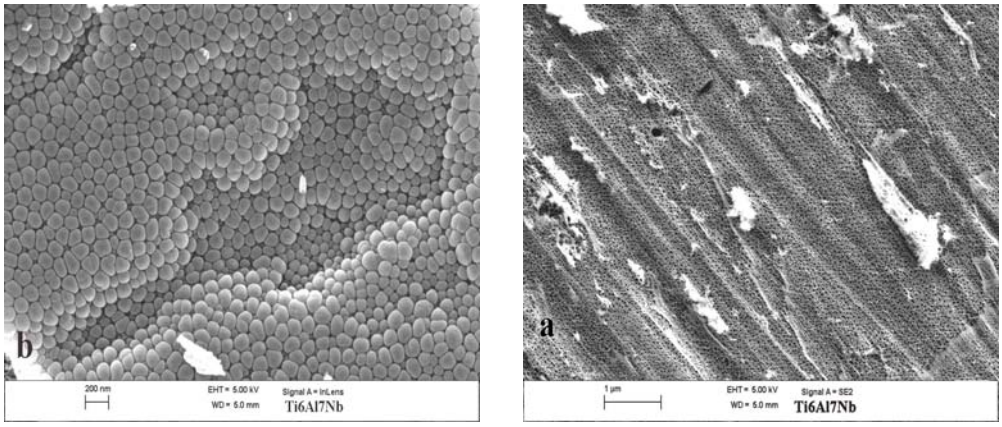

Fig.7. SEM image of Ti6Al7Nb surface after anodization in 1 M H_3PO_4 /0.2 wt% HF, for 40 minutes; (a) top view α and β phase; (b) bottom view

When the anodization time was increased to 1 hour, the α-phase surface was covered with a nanotubular oxide layer and the β-phase region with a random porous layer (Fig.8.).This type of morphology is specific to anodized α+β surface alloys [12-14]. Mean diameter of the nanotubes was around 70 nm and the mean wall thickness and intertube distance were around 20 nm and 108 nm, respectively. Nanotubular oxide layer was achieved in spite of a higher impact of water decomposition reaction (Fig.4, curve 2). The average nanotubes length was around 250 nm. In the SEM top view of the α-phase region (Fig.8, b) thin rings were observed on the top of the nanotubes. This phenomenon may be related with

the beginning of nanotubes dissolution, an aspect that was confirmed when the anodization time was increased up to 2 hours.

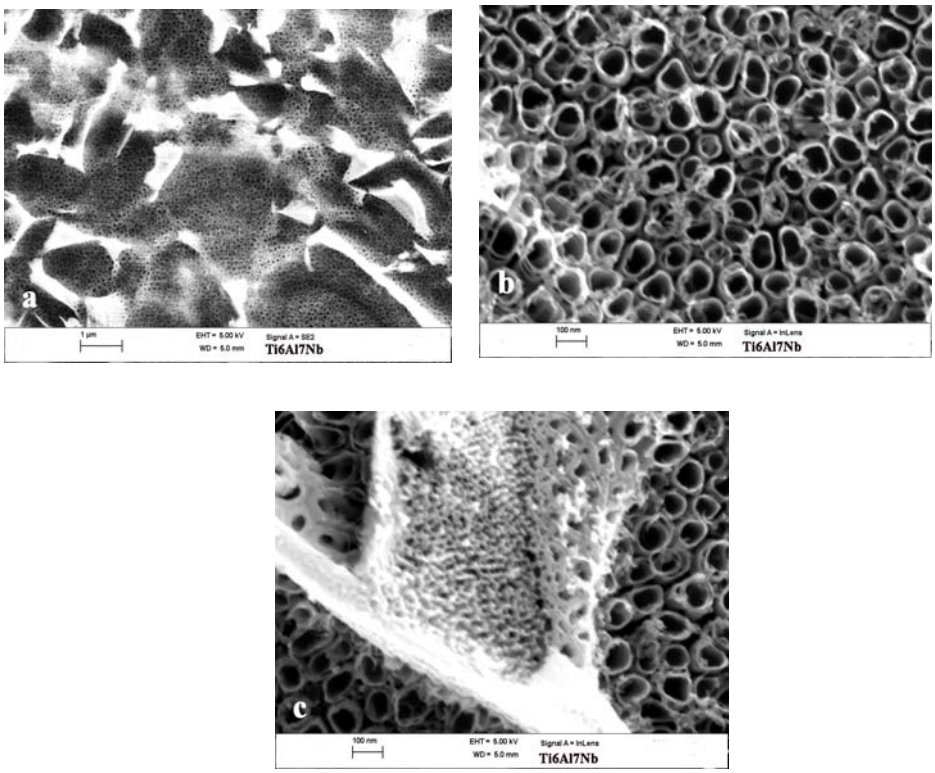

Fig.8. SEM image of Ti6Al7Nb surface after anodization in 1 M H_3PO_4 / 0.2 wt% HF, for 1 hour; (a) top view α-and β-phase; (b) top view α-phase; (c) top view β-phase;

After 2 hours both the α-and the β-phase regions seemed to be covered with a localized porous structure (Fig. 9, a, b). Meanwhile, in literature it was reported that a nanotubular and a porous layer region were achieved on α-phase and β-phase, respectively [14]. This difference between the results can be related to the higher Ti6Al7Nb nanotubes dissolution phenomenon in the employed electrochemical conditions. One may consider that on the Ti6Al7Nb surface a nanotubular oxide scale forms within the first hour of polarization. But it starts to dissolve in HF-containing solutions after prolonged anodization time. This effect is particularly pronounced in the electrolyte 2 with a higher HF concentration. The final surface structure established after 2 hours at 20 V can be assigned to an intermediate state between the nanotubes and nanopores.

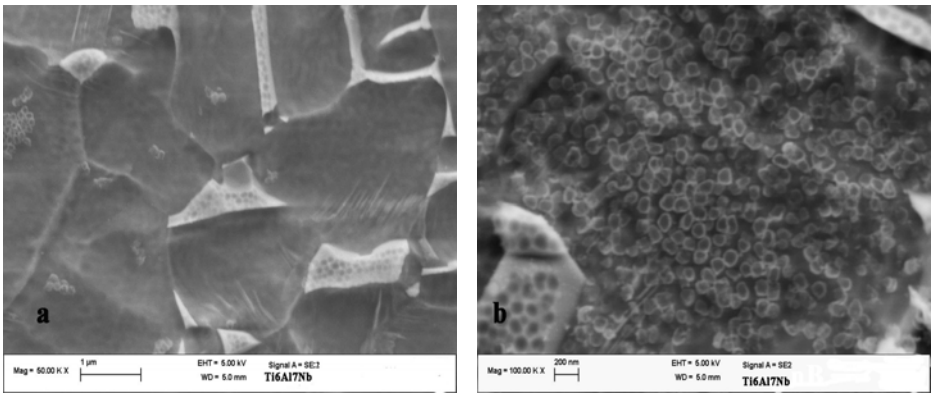

Fig.9. SEM image of Ti6Al7Nb surface after anodization in 1 M H_3PO_4+0.2 wt% HF, for 2 hour; (a) top view α and β phase; (b) top view α phase

4. Conclusions

The corrosion study showed that the investigated Ti6Al7Nb is stable in body fluid environment and its corrosion resistance is higher than for Ti.

Investigations regarding the anodization behavior of the α+β Ti6Al7Nb alloy were conducted in H_3PO_4/ 0.1 wt% HF and 0.2 wt% HF electrolytes applying a potential of 20 V for up to 2 hours potential and then sweeping the potential with 20 mV /s. Nanotubular oxide structures were obtained and it was demonstrated that the optimum polarization time is 1 hour for an 0.2 wt% HF concentration. The mean diameter and the length of the oxide nanotubes are about 70 nm and 250 nm, respectively. However, even when using the optimum anodization conditions, in the β-phase regions only random disordered nanoporous structures formed. This reveals the critical problem that α- and β-phases react very differently during the anodization processes. Furthermore, already after 2 hours anodization time no nanotubular or nanoporous layers were observed.

It can be concluded that employing the presented anodization parameters a nanotubular oxide structure was observed already after 1 hour in an electrolyte with higher HF concentration.

Acknowledgement

The work has been funded by the Sectoral Operational Programme Human Resources Development 2007-2013 of the Romanian Ministry of Labor, Family and Social Protection through the Financial Agreement POSDRU/88/1.5/S/61178.

REFERENCES

[1] *D.M.Brunette, P.Tengvall, M.Textor, P.Thomsen*, Titanium in Medicine, Springer, Berlin, 2001.
[2] *M.A.Imam, A.C.Fraker*, Titanium Alloys as Implant materials, ASTM Special Tehnical Publications 1272, 1996, pp.3-17.
[3] *M.M. Lohrengel*, Thin anodic oxide layers on aluminium and other valve metals: high field regime, Materials Science and Engineering**, R ll**, 1993, pp.243-294
[4] *S.Spriano, M.Vronzoni, E.Verne*, Journal of Bone and Joint Surgery, **87-B**, 2004.
[5] *MF Semlitsch, H. Weber, RM. Streicher, R. Schon*, Biomaterials, 1992, **13**, no.11, pp.781-8.
[6] *M.V.Popa, D.Raducanu, E.Vasilescu, P.Drob, D.Cojocaru, C.Vasilescu, S.Ivanescu, J.C.Mirza Rosca*, Materials and Corrosion, **59**, no.12, Dec.2008, pp.919-928.
[7] *K. Miura, N. Yamada, S. Hanada, T-K. Jung, Eiji Itoi*, Acta Biomaterialia, **7,** No.5, May 2011, pp 2320-2326.
[8] *X. Zhao, M. Niinomi, M. Nakai, G. Miyamoto, T. Furuhara*, Acta Biomaterialia, **7**, No.8, Aug. 2011, pp.3230-3236.
[9] *P.Laheurte, F.Prima, A.Eberhardt,T.Gloriant, M.Wary, E.Patoor* , Journal of the Mechanical Behavior of Biomedical Materials, **3**, No.8, Nov.2010,pp.565-573.
[10] *Z.Paszenda, W.Walke, S. Jadacka,* Journal of Achievements in Materials and Manufacturing Engineering, **39**, no.1, Jan. 2010, pp.24-34.
[11] *X. Liua, P/ K. Chub, C. Dinga*, Surface modification of titanium, titanium alloys and related materials for biomedical applications, Materials Science and Engineering, 2004, **R 47**, pp. 49–121
[12] *J.M.Macak, H.Tsuchiya, L.Taveira, A.Ghicov, P.Schmuki*, Journal of Biomedical A, Materials Research Part A, **75A**, no.4, Dec. 2005, pp.928-933.
[13] *M.Mîndroiu, C.Pirvu, R.Ion, I.Demetrescu*, Electrochimica Acta, **50**, no.1, Dec.2012, pp, 193-202.
[14] *A.Kaczmarek, T.Klekiel, E. Krasicka-Cydzik*, Surface and Interface analysis, **42**. no. 6-7, Jun.-Jul.2010, pp.510-514.
[15] *J.M.Macak, H. Tsuchiya, A.Ghicov, K.Yasuda, R.Hahn, Patrik Schumki*, Current Opinion in Solid State and Materials Sciencem **11**, no.1-2, Sept.2007, pp. 3-18.
[16] *S.E.Pust ,D.Scharnweber, C.N.Kirchner, G.Wittstock*, Advanced Materials, **19**, 2007, pp.878-882
[17] *G.A. Crawford, N. Chawla*, Acta Materialia**, 57**, no.3 , 2009, pp. 854–867.
[18] *G.K. Mor and Omman K. Varghese,* Journal of Materials Research, **18**, No. 11, 2003, pp.2588-2593.
[19] *P. Roy, S. Berger, P. Schmuki* , Angewandte Chemie International Edition, **50**, 2011, pp. 2904 – 2939.